



Since January 2020 Elsevier has created a COVID-19 resource centre with free information in English and Mandarin on the novel coronavirus COVID-19. The COVID-19 resource centre is hosted on Elsevier Connect, the company's public news and information website.

Elsevier hereby grants permission to make all its COVID-19-related research that is available on the COVID-19 resource centre - including this research content - immediately available in PubMed Central and other publicly funded repositories, such as the WHO COVID database with rights for unrestricted research re-use and analyses in any form or by any means with acknowledgement of the original source. These permissions are granted for free by Elsevier for as long as the COVID-19 resource centre remains active.

Generation and Selection of Coronavirus Defective Interfering RNA with Large Open Reading Frame by RNA Recombination and Possible Editing

YOUNG-NAM KIM,* MICHAEL M. C. LAI,† AND SHINJI MAKINO*¹

*Department of Microbiology, The University of Texas at Austin, Austin, Texas 78712; and †Howard Hughes Medical Institute and Department of Microbiology, University of Southern California, School of Medicine, Los Angeles, California 90033

Received November 13, 1992; accepted January 21, 1993

All of the coronavirus defective interfering (DI) RNAs analyzed thus far contain an open reading frame (ORF) from which DI RNA-specific protein(s) are translated, although the function of the DI-specific protein and the significance of the ORF are not known. A complete cDNA clone of a mouse hepatitis virus (MHV) DI RNA, NE-1, containing a single nucleotide deletion in the 5' region of the ORF was obtained and analyzed. Due to this single nucleotide deletion, a DI-specific protein of 7.5-kDa was made from NE-1, in contrast to the 88-kDa protein made from the wild-type DI RNA. NE-1 RNA was efficiently replicated after transfection into MHV-infected cells. However, after one passage of NE-1 RNA-containing virus, the 88-kDa wild-type protein was synthesized, indicating that the large ORF was restored during NE-1 DI RNA replication. Sequence analysis of NE-1 DI RNA from infected cells demonstrated that in approximately half of the DI RNA population, the ORF was restored by RNA recombination between NE-1 DI RNA and helper virus genomic sequence. The sequences of other DI RNAs contained an additional nontemplated A at the five-A sequence nine nucleotides upstream of the deletion site, resulting in a stretch of six consecutive As. In these "edited"-type DI RNAs, the original nucleotide deletion was maintained and no RNA recombination was observed. This "editing" produced an ORF of the same size as the wild-type DI RNA. We conclude that the DI RNA with a large ORF has a selective advantage. There was no significant difference in replication efficiency among these RNAs when they replicated alone. However, cotransfection of two DI RNA species and time course experiments suggested that homologous interference and other mechanism(s) during the early stage of virus multiplication are responsible for the accumulation of DI RNAs containing the large ORF. © 1993 Academic Press, Inc.

INTRODUCTION

Mouse hepatitis virus (MHV), a coronavirus, contains an approximately 31 kb-long genomic RNA (Lai and Stohman, 1978; Lee *et al.*, 1991; Pachuk *et al.*, 1989). In MHV-infected cells, seven to eight species of virus-specific subgenomic mRNAs with a 3'-coterminal nested-set structure (Lai *et al.*, 1981; Leibowitz *et al.*, 1981) are synthesized; these are numbered 1 to 7, in decreasing order of size (Lai *et al.*, 1981; Leibowitz *et al.*, 1981). None of the mRNAs are packaged into MHV virions, except for mRNA 1, which is efficiently packaged due to the presence of a packaging signal near the 3'-end of gene 1 (Fosmire *et al.*, 1992). The 5' end of MHV genomic RNA contains a 72- to 77-nucleotide-long leader sequence (Lai *et al.*, 1983, 1984; Spaan *et al.*, 1983). An identical sequence is found at the 5'-end of each MHV mRNA species; in each, the leader sequence is fused with the mRNA body sequence, which starts from a consensus sequence at each intergenic site (Makino *et al.*, 1988c; Shieh *et al.*, 1987).

Due to the large size of coronavirus genomic RNA, construction of its full-length, infectious cDNA clone

has not been successful. Instead, a system has been established in which complete cDNA clones of MHV defective interfering (DI) RNAs were placed downstream of T7 RNA polymerase promoters to generate DI RNAs capable of efficient replication in the presence of a helper virus. This system has been used for studying MHV RNA replication (Makino and Lai, 1989), transcription (Jeong and Makino, 1992; Joo and Makino, 1992; Makino *et al.*, 1991), RNA recombination (de Groot *et al.*, 1992; van der Most *et al.*, 1992), and packaging (Fosmire *et al.*, 1992; Makino *et al.*, 1990; van der Most *et al.*, 1991). MHV DI RNAs can be classified into three types. One is DI RNA of nearly genomic size, as exemplified by DIssA (Makino *et al.*, 1985), which is efficiently packaged into virus particles and replicates even in the absence of helper virus (Makino *et al.*, 1988a). The second type consists of smaller DI RNAs, which require helper virus infection for replication and are not packaged efficiently into MHV particles (Makino *et al.*, 1985, 1988a). The best-studied DI of this type is DIssE, which is the smallest MHV DI RNA found thus far (Makino *et al.*, 1988a,b). DIssE is 2.2 kb in length and consists of three noncontiguous genomic regions, comprising the first 0.86 kb from the 5'-end, an internal 0.75 kb from gene 1, which presumably en-

¹ To whom reprint requests should be addressed.

codes the virus-specific RNA polymerase, and 0.6 kb from the 3'-end of the parental MHV genome (Makino *et al.*, 1988b). The third type of DI RNA also requires helper virus infection for its replication; however, as it contains a packaging signal, it can be packaged efficiently (Makino *et al.*, 1990; van der Most *et al.*, 1991). The structure of the 3.6 kb-long DIssF, a prototype of the third type, consists of sequences derived from five noncontiguous regions of the genome of nondefective MHV (Makino *et al.*, 1990). The first four regions (domains I to IV) from the 5' end are derived from gene 1 and the 3'-most domain (domain V) is derived from the 3'-end of the genomic RNA. Both the second and third types of MHV-JHM-derived DI RNAs contain one large open reading frame (ORF) from which proteins are translated (Makino *et al.*, 1988b, 1990). Significantly, MHV-A59-derived DI RNAs also contain a large ORF (van der Most *et al.*, 1991). Thus, it seems that the presence of a large ORF is a common feature of MHV DI RNAs. Very recently, it was demonstrated that during serial passages of a series of MHV-A59-derived DI RNA mutants, each of which contained a truncated ORF, small truncated ORFs were converted into larger ORFs by RNA recombination during serial passage of DI particles (de Groot *et al.*, 1992), suggesting that DI RNAs containing a larger ORF have some advantage for accumulation, although the mechanism of accumulation of these DI RNAs is not known.

In the present study, we analyzed a DIssE-derived mutant DI RNA with a 1-nucleotide deletion at position 376 from the 5'-end. This 1-nucleotide deletion produces an ORF of one-tenth the size of the DIssE-specific ORF. The data obtained from this study demonstrated that DI RNA containing this small ORF can replicate at the same efficiency as DI RNA containing the large ORF. During RNA replication, however, DI RNA with the small ORF was replaced with novel DI RNAs containing the large ORF. Of this group, approximately half of the DI RNAs contained sequences created by RNA recombination and the remainder contained sequences in which a specific nucleotide was added at a specific site upstream of DI RNA nucleotide 376. Possible mechanisms for the efficient accumulation of DI RNAs containing the large ORF were studied.

MATERIALS AND METHODS

Viruses and cells

The plaque-cloned A59 strain of MHV (MHV-A59) was used as a helper virus. Mouse DBT cells (Hirano *et al.*, 1974) were used for RNA transfection and propagation of viruses.

RNA transcription and transfection

Plasmids were linearized by *Xba*I digestion and transcribed *in vitro* with T7 RNA polymerase as described

previously (Makino and Lai, 1989). The lipofection procedure used for RNA transfection was described previously (Makino *et al.*, 1991). The DI RNA transcribed *in vitro* was transfected into MHV-infected cells at 1 hr postinfection (p.i.). Viruses were harvested at 12 hr p.i. and passaged without dilution on fresh DBT cells. Virus samples obtained from DI RNA-transfected cells are referred to as passage 0 virus samples.

Preparation of virus-specific intracellular RNA

Intracellular virus-specific RNA was extracted as described previously (Makino *et al.*, 1984). For the study of negative-strand RNA, a slight modification of the extraction procedure described by Sawicki and Sawicki (1990) was used. Briefly, after washing the cells with ice-cold phosphate-buffered saline, cells were lysed with LET buffer (0.1 M LiCl, 0.01 M Tris-hydrochloride [pH 7.4], and 0.002 M EDTA) containing 50 mg of lithium dodecyl sulfate per milliliter and 200 μ g of proteinase K per milliliter. The solubilized cells were passed through a 19-gauge needle. After incubation at 37° for 30 min, samples were passed through a 27-gauge needle and extracted with phenol-chloroform. After ethanol precipitation, the samples were incubated with DNase I (0.5 U/ml) in a DNase buffer consisting of 100 mM NaCl, 10 mM Tris-hydrochloride (pH 7.8), 2 mM CaCl₂, and 2 mM MgCl₂ for 15 min at 30°. Intracellular RNA was extracted with phenol-chloroform and precipitated with ethanol.

Plasmid construction

Polymerase chain reaction (PCR) products which corresponded to the 5' end 1.5 kb region of DIssF were obtained as previously described (Makino *et al.*, 1990). Two cDNA clones, PCR-1 and PCR-2, were analyzed after the PCR products were cloned; the sequence of PCR-1 has been described (Makino *et al.*, 1990). The sequence of PCR-2 was identical to that of PCR-1 except for a 1-nucleotide deletion at position 376 from the 5'-end of PCR-2. Two complete DIssE-specific cDNA clones, NE and NE-1, were constructed by inserting the 1.5-kb *Sna*BI-*Spe*I fragments of PCR-1 and PCR-2, respectively, into the 2.9-kb *Sna*BI-*Spe*I fragment of DIssE-specific cDNA clone DE5-w4 (Makino *et al.*, 1989) (Fig. 1).

PCR

For the amplification of negative-stranded MHV RNA species, MHV-specific cDNA was first synthesized from intracellular RNA as previously described (Makino *et al.*, 1988b), using as a primer oligonucleotide 1567 (5'-CCTCTGCTGCGCAAGAA-3'), which binds to negative-strand DI RNA at nucleotides 332 to 348 from the 3'-end. After cDNA synthesis, reverse transcriptase was inactivated by heating the sample at 100° for 10

min. MHV-specific cDNA was then incubated with oligonucleotide 1568 (5'-TCTGCATATGCAACATC-3'), which binds to positive-sense DI RNA at nucleotides 871 to 887 from the 5'-end, in PCR buffer (0.05 M KCl, 0.01 M Tris-hydrochloride [pH 8.3], 0.0025 M MgCl₂, 0.01% gelatin, 0.17 mM each of dNTPs, and 5 U of Taq polymerase [Promega]) at 93° for 30 sec, 55° for 30 sec, and 72° for 100 sec for 25 cycles. For amplification of positive-stranded MHV RNA species, oligonucleotide 154 (5'-CTGCTCCCTGGCAACGCC-3'), which binds to positive-strand MHV DI RNA at nucleotides 952 to 966 from the 5'-end, was used for first-strand cDNA synthesis and oligonucleotide 52 (5'-AAGCTT-AATACGACTCACTATAGTATAAGAGTGATTGGCG-TCCGTAC-3') (Makino and Lai, 1989), which binds to negative-strand MHV genomic and DI RNAs at nucleotides 1 to 24 from the 3'-end, was added to the cDNA sample for subsequent PCR. The same PCR conditions described above were used.

Direct sequencing of the PCR product

Direct sequencing of the PCR product was performed according to the procedure described previously (Joo and Makino, 1992; Winship, 1989). An oligonucleotide 167 (5'-CTTCTGGGGATCCTCGTC-3') (Makino *et al.*, 1991), which binds to positive-sense DI RNA at nucleotides 452 to 469 from the 5'-end, was used as a primer.

Radiolabeling of viral RNAs and agarose gel electrophoresis

Virus-specific RNAs in virus-infected cells were labeled with ³²P_i as previously described (Makino *et al.*, 1984) and separated by electrophoresis on 1% agarose gels after denaturation with 1 M glyoxal (McMaster and Carmichael, 1977).

In vitro translation

An mRNA-dependent rabbit reticulocyte lysate (Promega) was used as previously described (Makino *et al.*, 1988b, 1990). *In vitro* translation using wheat germ extract (Promega) was used for the analysis of low molecular weight proteins.

Purification of viruses

After clarification of cell debris by low speed centrifugation of virus samples released from infected cells, MHV virion was purified by sucrose gradient centrifugation as previously described (Fosmire *et al.*, 1992).

Labeling of intracellular proteins, immunoprecipitation, and SDS-PAGE

Labeling of intracellular proteins, immunoprecipitation, and SDS-polyacrylamide gel electrophoresis

(PAGE) were performed as previously described (Makino *et al.*, 1985, 1990).

RESULTS

Restoration of MHV DI RNA ORF during NE-1 DI RNA replication

During sequence analysis of the cloned PCR products of DIssF DI RNA, we found that one of the cloned PCR products had a single A-nucleotide deletion at position 376 from the 5' end (Fig. 1). Due to this nucleotide deletion, the DI RNA-specific ORF was closed 6 nucleotides downstream of the deletion site. To test the ability of MHV DI RNA containing such a small ORF to replicate in MHV-infected cells, two complete DIssE-derived cDNA clones, NE and NE-1, were constructed. These clones contained identical sequences except that NE-1 had a single A deletion at nucleotide 376, producing a 57-amino-acid ORF. In contrast, the ORF of NE encoded 567 amino acids, similar to that of wild-type DIssE (Makino *et al.*, 1988b) (Fig. 1). To confirm that each DI RNA encoded its predicted ORF, plasmids NE and NE-1 were linearized with *Xba*I, and transcribed by T7 RNA polymerase in the presence of cap analog [m⁷G(5')ppp(5')G] (Makino *et al.*, 1989). *In vitro*-synthesized NE and NE-1 DI RNAs were then translated *in vitro*, and the proteins synthesized were examined directly by SDS-PAGE (Fig. 2A) and by immunoprecipitation of the products by anti-p28 antibody, which recognizes the N-terminus region of gene 1 products (Baker *et al.*, 1989) (Fig. 2B). A 7.5-kDa protein was translated from NE-1 DI RNA, consistent with its predicted molecular mass of 7308. In contrast, an 88-kDa protein was translated from NE DI RNA, and was specifically immunoprecipitated by the anti-p28 antibody. The size of this protein was identical to that of the DIssE translation product (Makino *et al.*, 1988b). Since the anti-p28 antibody recognizes the amino acid sequence encoded by nucleotides 437 to 484 from the 5'-end of MHV RNA (Fig. 1), and this sequence is not present in NE-1, the NE-1-specific 7.5-kDa protein was not precipitated by the anti-p28 antibody (data not shown). To confirm that the 7.5-kDa protein was indeed translated from the predicted ORF of NE-1, the cDNA of NE DI RNA was digested with *Nae*I, which cleaves NE cDNA at nucleotide 400 from the 5'-end, and the RNA was transcribed and translated. The size of the translated product was not different from that of the full-length NE-1 RNA (Fig. 2A). These analyses demonstrated that the 7.5-kDa and the 88-kDa proteins were translated from the predicted ORFs of NE-1 and NE DI RNA, respectively.

To determine if NE-1 DI RNA replicates in MHV-infected cells, equal amounts of *in vitro*-synthesized NE and NE-1 DI RNAs were independently transfected by lipofection into monolayers of DBT cells infected with

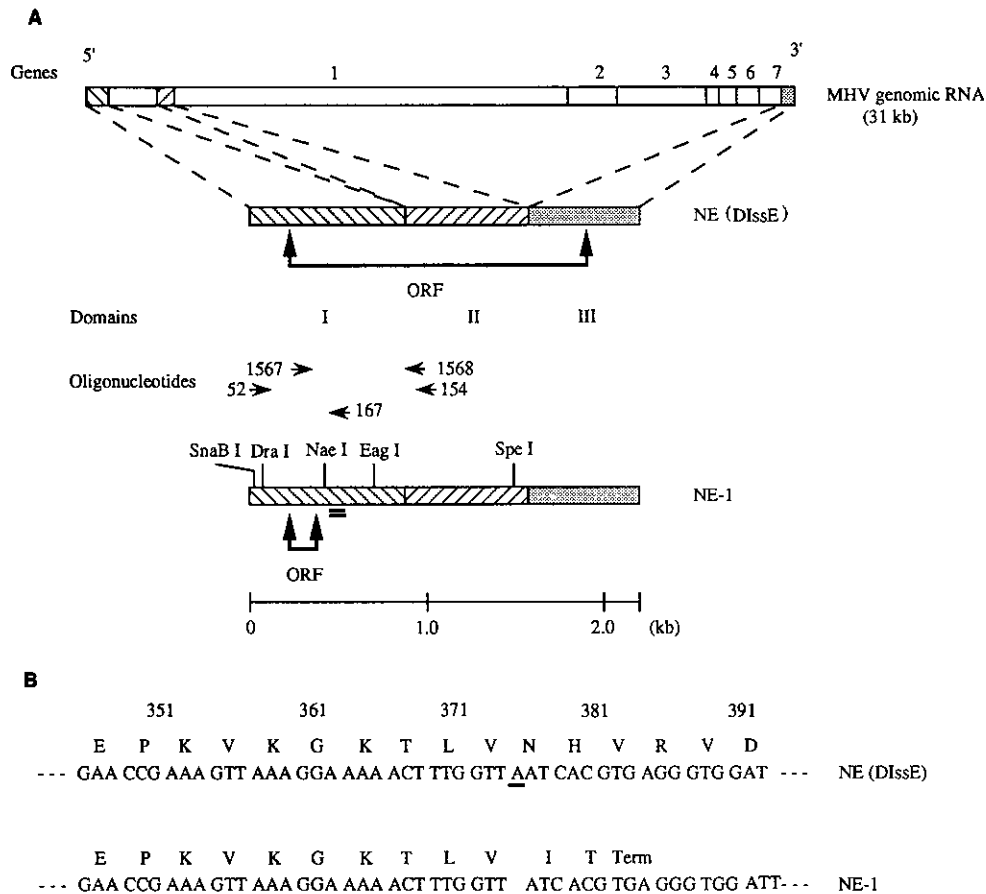


Fig. 1. Diagram of the structures of NE and NE-1. (A) Comparison of the structures of NE, NE-1, and standard MHV genomic RNA. Genes 1 through 7 represent the seven genes of MHV. The locations of the ORFs of NE and NE-1 are shown. The three domains of DIssE-derived DI RNAs (domains I through III) and the oligonucleotides used in the present study are indicated below the diagram of NE. The restriction enzyme sites are indicated above NE-1. The double-underlined region under NE-1 represents the region which is recognized by the anti-p28 antibody (2). (B) The nucleotide and deduced amino acid sequences of the 5'-regions of NE and NE-1. The numbers above these represent the nucleotide positions from the 5'-end of NE DI RNA. The A (underlined) in the NE sequence is missing from NE-1.

MHV-A59 helper virus 1 hr prior to transfection. The virus was harvested at 12 hr p.i. and used to infect DBT cells, and the ^{32}P -labeled intracellular RNA species obtained were analyzed by agarose gel electrophoresis. Efficient replication of both NE- and NE-1-derived DI RNAs was observed and there was no significant difference in the efficiency of RNA replication and accumulation between the two DI RNAs (Fig. 3a). To examine whether NE-1-derived DI RNA still contained the small ORF, metabolic labeling of MHV-specific proteins and subsequent immunoprecipitation of MHV-specific proteins by the anti-p28 antibody were performed. Virus-infected DBT cells were labeled with 100 $\mu\text{Ci/ml}$ of ^{35}S methionine for 20 min at 6.5 hr p.i. and the MHV-specific proteins were immunoprecipitated with the anti-p28 antibody and analyzed by SDS-PAGE. As shown in Fig. 3b, the synthesis of the 88-kDa protein was observed in NE DI RNA-transfected, MHV-infected cells as well as in cells infected with NE DI RNA-derived passage 0 virus sample. Surprisingly, the 88-kDa DI-specific protein was also detected in cells

infected with passage 0 virus sample obtained from NE-1 DI RNA-transfected cells, although it was not detected in the NE-1 RNA-transfected and MHV-infected cells. This result suggested that the small ORF present in the original NE-1 DI RNA was changed to the large ORF during DI RNA replication and amplification.

To confirm the change in the NE-1 ORF during RNA replication, sequence analysis of the DI RNA present in passage 0 virus-infected cells was performed. Intracellular RNA was extracted at 7 hr p.i. from cells infected with passage 0 virus samples obtained from NE-1 DI RNA-transfected, MHV-infected cells. MHV-specific cDNA was synthesized from the intracellular RNAs using oligonucleotide 154 as a primer, which binds at nucleotides 3200 to 3218 from the 5'-end of MHV genomic RNA (Lee *et al.*, 1991), corresponding to nucleotides 951 to 966 from the 5'-end of DIssE RNA (Fig. 1). After cDNA synthesis, cDNA was mixed with oligonucleotide 52 (Makino and Lai, 1989), which binds to the leader sequence of negative-stranded MHV RNA, and 25 cycles of PCR were performed. A DI RNA-specific

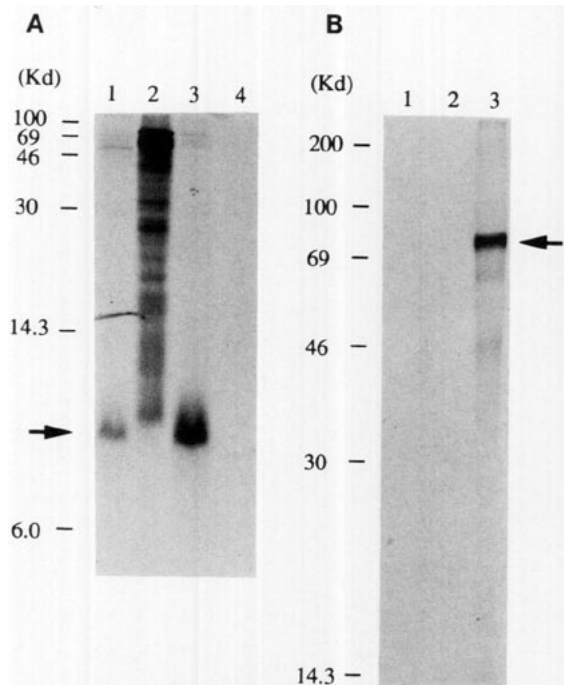


FIG. 2. (A) *In vitro* translation of NE and NE-1-specific proteins. SDS-PAGE of the *in vitro* translation products of NE-1 (lane 1), NE (lane 2), the 400-nucleotide-long 5'-region of NE RNA (lane 3), and no RNA (lane 4). Translation was performed in a wheat germ extract system, using [³⁵S]methionine. (B) *In vitro* translation and immunoprecipitation of NE and NE-1-specific proteins. *In vitro* translation of NE-1 (lane 2), NE (lane 3), and no RNA (lane 1) was performed in a rabbit reticulocyte lysate system, using [³⁵S]methionine. *In vitro* translation products were immunoprecipitated with anti-p28 antibody and analyzed by SDS-PAGE.

PCR product with the predicted size of 0.96 kb was obtained (data not shown). The PCR product was digested with *Dra*I and *Eag*I and the gel-purified 0.65 kb-long DI RNA-specific PCR product was cloned into a plasmid vector and sequenced. This experiment was conducted twice independently, under identical conditions, with virtually no difference in sequencing results (Fig. 4). Sequence analysis of the 36 clones obtained demonstrated that the sequences of DI RNAs in passage 0 virus-infected cells could be classified into three types. Eighteen of the 36 clones had a sequence in which the A nucleotide deletion at position 376 was repaired; these clones also contained A59-derived sequence downstream at positions 391, 411, and 432. As it is known that MHV undergoes high-frequency RNA recombination (Baric *et al.*, 1990; Makino *et al.*, 1986), it seems likely that this sequence alteration was probably caused by RNA recombination between NE-1 DI RNA and MHV-A59 helper virus genomic RNA. The second type was represented by one clone, which demonstrated a similar sequence alteration by RNA recombination, but its G nucleotide at position 140 was also replaced by the MHV-A59 A nucleotide, suggesting multiple cross-overs. In the remaining 17 clones, the single A nucleotide deletion at position 376 was

not repaired and no RNA recombination was observed. However, each of these clones contained an additional A insertion 9 nucleotides upstream of the deletion site; this insertion produced a stretch of 6 consecutive As. This nucleotide addition converted the NE-1-specific small ORF into a long ORF encoding 567 amino acids. The ORF made from these clones contained a contiguous 4-amino-acid sequence which was different from that of NE DI RNA (Fig. 5). These sequence analyses clearly demonstrated that in the passage 0 virus-infected cells, NE-1 DI RNA was replaced by two different DI RNA species, one of which was created by RNA recombination and the other DI RNA by "editing" of the RNA sequence, although we do not know whether the latter type RNA was derived *de novo* in the cells or generated from *in vitro* transcription.

Analysis of accumulation mechanisms of DI RNA containing the large ORF

To understand the mechanism of the efficient accumulation of DI RNA containing the large ORF, a cDNA

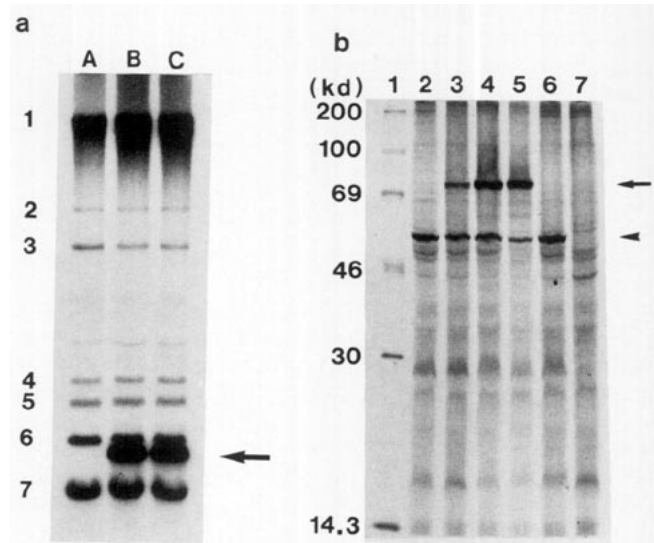


FIG. 3. Replication and protein synthesis by NE and NE-1 DI RNA in passage 0 virus-infected cells and RNA-transfected cells. (a) Agarose gel electrophoresis of MHV-specific intracellular RNAs which were obtained after infection of passage 0 virus samples. ³²P-labeled virus-specific RNA from DBT cells infected with MHV-A59 (lane A), passage 0 virus samples obtained from NE-transfected cells (lane B), or from NE-1-transfected cells (lane C) was denatured with glyoxal and electrophoresed on a 1% agarose gel. Numbers 1 to 7 denote MHV-specific mRNA species. The arrow indicates DI RNAs. (b) SDS-PAGE of proteins from DI RNA-replicating cells. DBT cells were infected with MHV-A59 and transfected with *in vitro*-synthesized NE-1 DI RNA (lane 2), NE DI RNA (lane 3), or mock-transfected (lane 6). DBT cells were infected with passage 0 virus samples obtained from NE-1 DI RNA-transfected cells (lane 4), or from NE DI RNA-transfected cells (lane 5). Lane 7 represents mock-infection and mock-transfection. At 6.5 hr p.i., cultures were labeled with [³⁵S]methionine for 20 min; total cell extracts were then prepared and immunoprecipitated with anti-p28 antibody. The 88-kDa DI-specific protein is indicated by the arrow. The band indicated by the arrowhead represents the nucleocapsid protein of MHV-A59. Lane 1, ¹⁴C-labeled marker proteins.

	129	140	180	361	371		381	391	411	432		
					↓							
	A	A	G	AAGGAAAAACUUUGGUUAAUCAC			A	U	U		MHV-A59	
	C	G	C	AAGGAAAAACUUUGGUUAAUCAC			G	C	C		MHV-JHM	
	C	G	C	AAGGAAAAACUUUGGUUA			UCAC	G	C	C	NE-1	
											Exp. 1	
											Exp. 2	
											Total	
	C	G	C	AAGGAAAAACUUUGGUUAAUCAC			<u>A</u>	<u>U</u>	<u>U</u>		Recombinant type 1	6 clones
	C	<u>A</u>	C	AAGGAAAAACUUUGGUUAAUCAC			<u>A</u>	<u>U</u>	<u>U</u>		Recombinant type 2	0 clone
	C	G	C	AAGGAAAA <u>AA</u> CUUUGGUUAAUCAC			G	C	C		Edited type	4 clones
											Total	10 clones
											26 clones	36 clones

FIG. 4. Sequences of cloned PCR products of DI RNAs derived from cells infected with passage 0 virus sample obtained from NE-1 DI RNA-transfected, MHV-infected cells. MHV-A59, MHV-JHM, and NE-1 sequences are also shown for comparison. Nucleotide positions numbered from the 5'-end of the genome are shown above the MHV-A59 sequence. Underlined nucleotides indicate MHV-A59-specific nucleotides. The A nucleotide inserted into the edited DI RNA is indicated by double underlining. The number of clones used for sequence analysis in each of the two independent experiments are listed under Exp. 1 and Exp. 2.

clone, NE-2, was constructed, which has a sequence identical to NE-1 except for an additional A nucleotide at position 368 of NE-2 (Fig. 5); thus, NE-2 DI RNA had the same sequence as the "edited"-type DI RNA. To examine whether DI RNA containing the large ORF replicated more efficiently than NE-1 DI RNA, the replication efficiencies of NE DI RNA, NE-1 DI RNA, and NE-2 DI RNA were compared. Equal amounts of each *in vitro*-synthesized DI RNA were transfected separately into MHV-A59-infected cells, and MHV-specific intracellular RNA species were labeled with ^{32}P from 5 to 7 hr p.i. The RNAs were extracted and then separated by an agarose gel electrophoresis (Fig. 6). The quantity of DI RNA was estimated by densitometric scanning of the autoradiograms. There was no significant difference in the efficiency of RNA replication and accumulation among the three DI RNAs. This result was reproduced in three independent experiments. These data suggested that the accumulation of the DI RNAs containing the large ORF was not due to a greater efficiency of replication of the DI RNAs containing the large ORF.

We then examined whether DI RNA containing the large ORF interferes with the replication of NE-1 DI RNA. For this analysis three RNA samples were prepared, one consisting of 99% NE-1 and 1% NE-2, one consisting of 90% NE-1 and 10% NE-2, and a third sample consisting of 50% NE-1 and 50% NE-2. Each RNA mixture was transfected into MHV-A59-infected DBT cells, and total RNA extracted at 7 hr p.i. It has previously been demonstrated that two different RNA molecules can be efficiently cointroduced into MHV-infected cells using this RNA transfection condition (Jeong and Makino, 1992). This total RNA was then used for cDNA synthesis and amplification. To avoid detection of the amplified input DI RNAs, which were still present in small quantity as late as 6 hr post-transfection in the DI RNA-transfected cells (Jeong and Makino, 1992), we examined the accumulation of negative-stranded RNA. MHV negative-strand RNA-derived cDNA was initially synthesized using oligonucleotide 1567, which specifically binds to negative-stranded DI RNAs at nucleotides 332 to 348 from the 3'-end. After cDNA synthesis, reverse transcriptase was inactivated

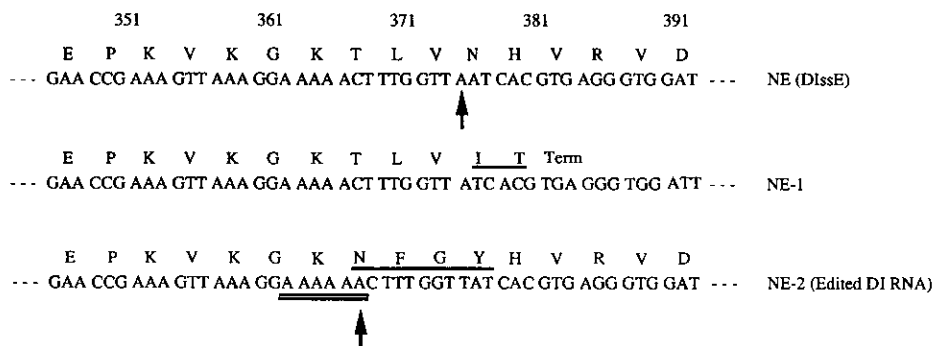


FIG. 5. Nucleotide and deduced amino acid sequence comparison of NE, NE-1 and NE-2. Amino acid sequences which differ from NE are indicated by underlining. The A nucleotide missing from NE-1 is shown by an arrow in the NE sequence. The A nucleotide added to NE-2 is shown by an arrow in the NE-2 sequence. The stretch of six consecutive A nucleotides are shown by double underlining.

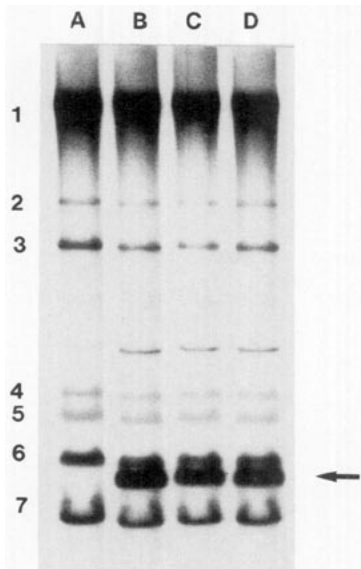


Fig. 6. Replication of NE, NE-1, and NE-2 DI RNAs in DI RNA-transfected cells. DBT cells were infected with MHV-A59 1 hr prior to transfection of NE DI RNA (lane B), NE-1 DI RNA (lane C), NE-2 DI RNA (lane D), or mock-transfection (lane A). Virus-specific RNA species were labeled with ^{32}P , from 5 to 7 hr p.i. and the extracted RNA was denatured with glyoxal and electrophoresed on a 1% agarose gel. Numbers 1 to 7 represent MHV-specific mRNA species. DI RNAs are indicated by the arrow.

by heating the sample at 100° for 10 min, oligonucleotide 1568 was added to the sample, and PCR was performed. Oligonucleotide 1568 hybridizes to positive-strand DI RNA at nucleotides 871 to 887 from the 5' end, and to MHV genomic RNA at nucleotides 3119 to 3135 from the 5'-end. The DI RNA-specific PCR product of 0.5 kb was clearly generated by this PCR reaction, whereas the 2.8 kb-long negative-stranded MHV genomic RNA-specific PCR product was not detected (data not shown). The specificity of these reactions was demonstrated by repeating the reverse transcription and amplification procedure described above, using a sample containing a mixture of *in vitro*-synthesized NE-1 DI RNA and intracellular RNA species from MHV-A59-infected cells. In this case, the synthesis of a DI RNA-specific PCR product was not observed (data not shown). Direct sequencing of the gel-purified DI RNA-specific PCR product demonstrated that it contained 5 As, which is identical to NE-1 DI RNA, when the transfected samples contained 99% NE-1 and 1% NE-2, or 90% NE-1 and 10% NE-2. The NE-2 DI RNA-specific sequence, which contained 6 As, was not apparent in either sequencing analysis (Fig. 7). Direct sequencing of the PCR products obtained from cells cotransfected with equal amounts of the two DI RNAs demonstrated that the majority of the DI RNA produced contained NE-2-derived sequence (Fig. 7). No apparent sequence heterogeneity was observed upstream of the 6-A stretch, demonstrating that DI RNA contain-

ing NE-1-specific sequence was a very minor population at 6 hr post-transfection. A similar result was obtained when equal amounts of NE RNA and NE-1 RNA were cotransfected into MHV-infected cells: the majority of the replicating DI RNA species at 6 hr post-transfection was NE DI RNA (data not shown). As a negative control, NE-1 DI RNA and NE-2 DI RNA were independently transfected into MHV-A59-infected cells, and PCR products were obtained from the intracellular RNA species of each using the procedure detailed above. Direct sequencing of these PCR products demonstrated that each DI RNA kept its original sequence at 6 hr post-transfection. These analyses suggested that one of the mechanisms of accumulation of DI RNA species containing the large ORF was homologous interference between DI RNAs containing the large ORF and NE-1 DI RNA, although the homologous interference activity was not very efficient.

Next to be examined was when the DI RNAs containing the large ORF became the major population during DI RNA replication. NE-1 DI RNA was transfected into MHV-A59-infected DBT cells 1 hr p.i., and intracellular RNA was extracted at 3, 6, and 12 hr p.i. The DI RNA from NE-1 RNA-transfected cells was analyzed by direct sequencing of the negative-stranded RNA-derived PCR product, as described above. Virion RNA and intracellular RNA from passage 0 virus-infected cells were also analyzed by direct sequencing of the positive-stranded RNA-derived PCR products. These studies demonstrated that the sequences of DI RNA from NE-1 RNA-transfected cells and passage 0 virus were identical to that of NE-1 (Fig. 8); recombinant and edited type DI RNA sequences were not detected; thus, they were not selectively packaged into virions. However, DI RNA in passage 0 virus-infected cells at 3 hr p.i. clearly contained mostly the recombinant type sequence, which have two A at nucleotides 376 and 377, but neither edited-type RNA nor parental DI RNA (Fig. 8). In contrast, sequences of DI RNA from passage 0 virus-infected cells at 6 hr p.i. had not only two A nucleotides at nucleotides 376 and 377 but also an additional A nucleotide inserted at 9 nucleotides upstream. Furthermore, the sequence between these two sites were heterogeneous, indicating that both recombinant- and edited-type DI RNAs were present at 6 hr p.i. in the passage 0 virus-infected cells. These results indicated that the DI RNA containing a large ORF accumulated only after one virus passage, and that the recombinant DI RNA accumulated earlier while the edited type DI RNA accumulated later in virus infection. The precise mechanism is not yet clear. Two independent experiments were performed and essentially the same results were obtained.

DISCUSSION

The present study demonstrated that DIssE-derived NE-1 DI RNA, which had a small ORF as compared to

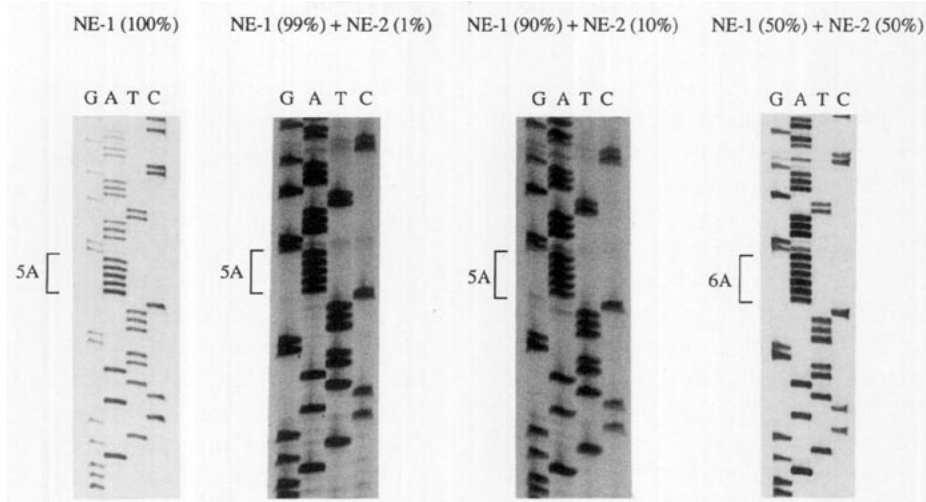


FIG. 7. Direct sequencing of the DI-specific PCR products synthesized from DI RNA-transfected, MHV-infected cells. *In vitro*-synthesized NE-1 and NE-2 DI RNAs were mixed at a molar ratio of 99 to 1, 90 to 10, or 50 to 50 in the transfection buffer, as indicated. The mixture of DI RNA samples were transfected into MHV-infected cells and total RNA was extracted at 7 hr p.i. DI-specific PCR products amplified from negative-stranded DI RNA were sequenced.

wild-type DIssE, replicated efficiently in MHV-infected cells. However, NE-1 RNA was found to synthesize a wild-type 88-kDa protein after 2 rounds of virus replication. Most of DI RNAs in passage 0 virus-infected cells contained a large ORF similar to that of wild-type DI RNA, and all had altered RNA structures. Approximately half of the DI RNAs were derived by RNA recombination, which removed the nucleotide deletion, supporting the hypothesis that RNA recombination is an important mechanism for the maintenance of MHV genome integrity, and that it plays a role in the evolution

of the coronavirus genome (Lai, 1992). The remainder, edited-type DI RNA, contained sequences in which an A nucleotide was inserted 9 nucleotides upstream of the deletion site. Although it is not known whether the addition of an A nucleotide at this specific site on DI RNA occurred during *in vitro* transcription of NE-1 RNA by T7 RNA polymerase or during replication of NE-1 DI RNA, this study suggests the advantage of a large ORF in MHV DI RNA replication.

It is evident that a large ORF is not necessary for DI RNA replication and accumulation, because NE-1 DI

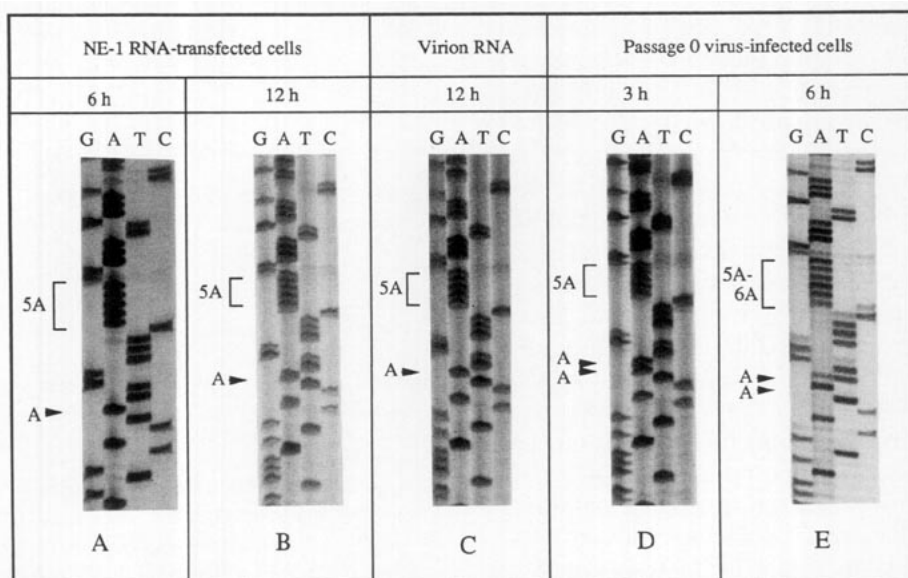


FIG. 8. Direct sequencing of the DI-specific PCR products synthesized from DI RNA-transfected, MHV-infected cells, purified DI particles and passage 0 virus-infected cells. *In vitro*-synthesized NE-1 was transfected into MHV-infected cells and total RNA was extracted at 6 hr (A) and 12 hr (B) p.i. Virion RNA was extracted from MHV particles which was harvested at 12 hr p.i. of NE-1-transfected cells (C). Intracellular RNA was extracted from the passage 0 virus-infected cells at 3 hr (D) and 6 hr p.i. (E).

RNA, with an ORF only one-tenth the size of the ORF of DIssE, replicated efficiently. If the DI-specific protein is necessary for DI RNA replication at all, the data presented here suggest that the N terminus of this protein is sufficient. It has been demonstrated that poliovirus DI RNA replication requires a large ORF (Collis *et al.*, 1992; Hagino-Yamagishi and Nomoto, 1989; Kaplan and Racaniello, 1988), and that all naturally occurring defective RNAs derived from the clover yellow mosaic virus (CYM), a potexvirus, also contain a large ORF (White *et al.*, 1992). The presence of a defective RNA-specific protein was demonstrated in CYM defective RNA-replicating cells (White *et al.*, 1992), and site-directed mutagenesis analysis indicated that the large ORF is necessary for the accumulation of the defective RNAs of this virus. The MHV DI RNA requirement is clearly different.

Our present study showed that DI RNAs with a large ORF accumulated during DI RNA replication. This observation was consistent with the recent analysis of MHV-A59-derived DI RNA ORF (de Groot *et al.*, 1992). We further demonstrated that the accumulation of the DI RNA with a large ORF was not due to a greater efficiency of replication of this type of DI RNAs but rather due to homologous interference between the DI RNAs containing the large ORF and NE-1 DI RNA (Fig. 7). Although the mechanism of homologous interference is not known, several possibilities may be considered. Due to the one-nucleotide deletion, the secondary or tertiary structures of NE-1 DI RNA might differ slightly from those of DI RNAs with the large ORF. It is possible that the MHV RNA replication machinery has a slightly better affinity for DI RNAs with the large ORF than for NE-1 DI RNA, resulting in the preferential replication of DI RNAs with the large ORF. The possible structural differences between these DI RNAs may be caused by the association of DI RNAs with ribosomes. It is conceivable that nascent positive-stranded DI RNA associates with ribosomes immediately after transcription and the DI-specific protein is synthesized cotranscriptionally. If this is the case, nascent strands of NE-1 DI RNA will dissociate from the ribosome at 0.38 kb from the 5'-end, while nascent strands of DI RNAs with the large ORF are associated with ribosome to 1.9 kb from the 5'-end. This difference may result in structural differences between different DI RNAs, and the RNA structure made by the longer association with ribosomes may have a better affinity for the RNA replication components. It has been proposed that a protein complex composed of viral and host proteins interacts with the 5'-region of nascent positive-stranded RNA, and this interaction is important for the replication of some positive-stranded RNA viruses (Andino *et al.*, 1990; Pogue and Hall, 1992). It is possible that coronavirus positive-stranded RNA synthesis has a similar regulation in which the 5'-region of the nascent positive-

stranded RNA is recognized by the viral RNA replication machinery.

Our study also showed that the DI RNAs with the large ORF did not accumulate until one round of virus passage. However, the DI RNAs containing a large ORF were not selectively packaged into MHV virion. Surprisingly, within the first 3 hr of infection, the recombinant DI RNA became the major species in the infected cells and the edited type RNA accumulated later at 6 hr. This observation is intriguing because efficient accumulation of the DI RNAs containing the large ORF was not observed when MHV-infected cells were transfected with RNA samples containing as much as 10% NE-2 RNA. Thus, the efficient accumulation of the DI RNA containing the large ORF may be triggered by the early steps of virus multiplication, such as virus penetration, uncoating, and initial translation prior to RNA replication. Since the incoming MHV RNA will be used for translation of RNA polymerase before RNA synthesis can take place, DI RNAs containing a large ORF may be associated with the translation machinery and, in some way, better utilized for RNA synthesis. This process may be related to virus penetration and the uncoating process. As yet, we do not know the reason for the differential rates of accumulation for the recombinant and edited type DI RNAs. Further studies are necessary to identify the mechanism(s) which are important for the accumulation of DI RNAs containing the large ORF.

ACKNOWLEDGMENTS

We thank Susan Baker for the anti-p28 antibody and Sima Vafaei for technical assistance. We thank Jennifer Fosmire for critical reading of the manuscript. This work was supported by Public Health Service Grants AI29984 (to S.M.) and AI16144 (to M.M.C.L.) from the National Institutes of Health. M.M.C.L. is an investigator of Howard Hughes Medical Institute.

REFERENCES

- ANDINO, R., RIECKHOF, G. E., and BALTIMORE, D. (1990). A functional ribonucleoprotein complex forms around the 5' end of poliovirus RNA. *Cell* **63**, 369-380.
- BAKER, S. C., SHIEH, C.-K., SOE, L. H., CHANG, M.-F., VANNIER, D. M., and LAI, M. M. C. (1989). Identification of a domain required for autoproteolytic cleavage of murine coronavirus gene A polyprotein. *J. Virol.* **63**, 3693-3699.
- BARIC, R. S., FU, K., SCHAAD, M. C., and STOHLMAN, S. A. (1990). Establishing a genetic recombination map for murine coronavirus strain A59 complementation groups. *Virology* **177**, 646-656.
- COLLIS, P. S., O'DONNELL, B. J., BARTON, D. J., ROGERS, J. A., and FLANEGAN, J. B. (1992). Replication of poliovirus RNA and subgenomic RNA transcripts in transfected cells. *J. Virol.* **66**, 6480-6488.
- DE GROOT, R. J., VAN DER MOST, R. G., and SPAAN, W. J. M. (1992). The fitness of defective interfering murine coronavirus DI-a and its derivatives is decreased by nonsense and frameshift mutations. *J. Virol.* **66**, 5898-5905.
- FOSMIRE, J. A., HWANG, K., and MAKINO, S. (1992). Identification and characterization of a coronavirus packaging signal. *J. Virol.* **66**, 3522-3530.

- HAGINO-YAMAGISHI, K., and NOMOTO, A. (1989). *In vitro* construction of poliovirus defective interfering particles. *J. Virol.* **63**, 5386–5392.
- HIRANO, N., FUJIWARA, K., HINO, S., and MATSUMOTO, M. (1974). Replication and plaque formation of mouse hepatitis virus (MHV-2) in mouse cell line DBT culture. *Arch. Gesamte Virusforsch.* **44**, 298–302.
- JEONG, Y. S., and MAKINO, S. (1992). Mechanism of coronavirus transcription: duration of primary transcription initiation activity and effect of subgenomic RNA transcription on RNA replication. *J. Virol.* **66**, 3339–3346.
- JOO, M., and MAKINO, S. (1992). Mutagenic analysis of the coronavirus intergenic consensus sequence. *J. Virol.* **66**, 6330–6337.
- KAPLAN, G., and RACANIELLO, V. R. (1988). Construction and characterization of poliovirus subgenomic replicons. *J. Virol.* **62**, 1687–1696.
- LAI, M. M. C. (1992). RNA recombination in animal and plant viruses. *Microbiol. Rev.* **56**, 61–79.
- LAI, M. M. C., BARIC, R. S., BRAYTON, P. R., and STOHLMAN, S. A. (1984). Characterization of leader RNA sequences on the virion and mRNAs of mouse hepatitis virus, a cytoplasmic RNA virus. *Proc. Natl. Acad. Sci. USA* **81**, 3626–3630.
- LAI, M. M. C., BRAYTON, P. R., ARMEN, R. C., PATTON, C. D., PUGH, C., and STOHLMAN, S. A. (1981). Mouse hepatitis virus A59: mRNA structure and genetic localization of the sequence divergence from hepatotropic strain MHV-3. *J. Virol.* **39**, 823–834.
- LAI, M. M. C., PATTON, C. D., BARIC, R. S., and STOHLMAN, S. A. (1983). Presence of leader sequences in the mRNA of mouse hepatitis virus. *J. Virol.* **46**, 1027–1033.
- LAI, M. M. C., and STOHLMAN, S. A. (1978). RNA of mouse hepatitis virus. *J. Virol.* **26**, 236–242.
- LEE, H.-J., SHIEH, C.-K., GORBALENYA, A. E., EUGENE, E. V., LA MONICA, N., TULER, J., BAGDZHADZHAN, A., and LAI, M. M. C. (1991). The complete sequence (22 kilobases) of murine coronavirus gene 1 encoding the putative proteases and RNA polymerase. *Virology* **180**, 567–582.
- LEIBOWITZ, J. L., WILHELMSSEN, K. C., and BOND, C. W. (1981). The virus-specific intracellular RNA species of two murine coronaviruses: MHV-A59 and MHV-JHM. *Virology* **114**, 39–51.
- MAKINO, S., FUJIOKA, N., and FUJIWARA, K. (1985). Structure of the intracellular defective viral RNAs of defective interfering particles of mouse hepatitis virus. *J. Virol.* **54**, 329–336.
- MAKINO, S., KECK, J. G., STOHLMAN, S. A., and LAI, M. M. C. (1986). High-frequency RNA recombination of murine coronaviruses. *J. Virol.* **57**, 729–737.
- MAKINO, S., JOO, M., and MAKINO, J. K. (1991). A system for study of coronavirus mRNA synthesis: A regulated, expressed subgenomic defective interfering RNA results from intergenic site insertion. *J. Virol.* **65**, 6031–6041.
- MAKINO, S., and LAI, M. M. C. (1989). High-frequency leader sequence switching during coronavirus defective interfering RNA replication. *J. Virol.* **63**, 5285–5292.
- MAKINO, S., SHIEH, C.-K., KECK, J. G., and LAI, M. M. C. (1988a). Defective-interfering particles of murine coronaviruses: Mechanism of synthesis of defective viral RNAs. *Virology* **163**, 104–111.
- MAKINO, S., SHIEH, C.-K., SOE, L. H., BAKER, S. C., and LAI, M. M. C. (1988b). Primary structure and translation of a defective interfering RNA of murine coronavirus. *Virology* **166**, 550–560.
- MAKINO, S., SOE, L. H., SHIEH, C.-K., and LAI, M. M. C. (1988c). Discontinuous transcription generates heterogeneity at the leader fusion sites of coronavirus mRNAs. *J. Virol.* **62**, 3870–3873.
- MAKINO, S., TAGUCHI, F., HIRANO, N., and FUJIWARA, K. (1984). Analysis of genomic and intracellular viral RNAs of small plaque mutants of mouse hepatitis virus, JHM strain. *Virology* **139**, 138–151.
- MAKINO, S., YOKOMORI, K., and LAI, M. M. C. (1990). Analysis of efficiently packaged defective interfering RNAs of murine coronavirus: Localization of a possible RNA-packaging signal. *J. Virol.* **64**, 6045–6053.
- MCMASTER, G. K., and CARMICHAEL, G. G. (1977). Analysis of single- and double-stranded nucleic acids on polyacrylamide and agarose gels by using glyoxal and acridine orange. *Proc. Natl. Acad. Sci. USA* **74**, 4835–4838.
- PACHUK, C. J., BREDBENBEEK, P. J., ZOLTICK, P. W., SPANN, W. J. M., and WEISS, S. R. (1989). Molecular cloning of the gene encoding the putative polymerase of mouse hepatitis virus, strain A59. *Virology* **171**, 141–148.
- POGUE, G. P., and HALL, C. T. (1992). The requirement for a 5' stem-loop structure in brome mosaic virus replication supports a new model for viral positive-strand RNA initiation. *J. Virol.* **66**, 674–684.
- SAWICKI, S. G., and SAWICKI, D. L. (1990). Coronavirus transcription: Subgenomic mouse hepatitis virus replicative intermediates function in RNA synthesis. *J. Virol.* **64**, 1050–1056.
- SHIEH, C.-K., SOE, L. H., MAKINO, S., CHANG, M.-F., STOHLMAN, S. A., and LAI, M. M. C. (1987). The 5'-end sequence of the murine coronavirus genome: Implications for multiple fusion sites in leader-primed transcription. *Virology* **156**, 321–330.
- SPAAN, W., DELIUS, H., SKINNER, M., ARMSTRONG, J., ROTTIER, P., SMEEKENS, S., VAN DER ZEIJST, B. A. M., and SIDDELL, S. G. (1983). Coronavirus mRNA synthesis involves fusion of non-contiguous sequences. *EMBO J.* **2**, 1939–1944.
- VAN DER MOST, R. G., BREDBENBEEK, P. J., and SPAAN, W. J. M. (1991). A domain at the 3' end of the polymerase gene is essential for encapsidation of coronavirus defective interfering RNAs. *J. Virol.* **65**, 3219–3226.
- VAN DER MOST, R. G., HEIJNEN, L., SPAAN, W. J. M., and DE GROOT, R. J. (1992). Homologous RNA recombination allows efficient introduction of site-specific mutations into the genome of coronavirus MHV-A59 via synthetic co-replicating RNAs. *Nucleic Acids Res.* **20**, 3375–3381.
- WHITE, K. A., BANCROFT, J. B., and MACKIE, G. A. (1992). Coding capacity determines *in vivo* accumulation of a defective RNA of clover yellow mosaic virus. *J. Virol.* **66**, 3069–3076.
- WINSHIP, P. R. (1989). An improved method for directly sequencing PCR material using dimethyl sulfoxide. *Nucleic Acids Res.* **17**, 1266.